FULL PAPERS

Magnetic Resonance in Medicine 63:303–311 (2010)

High-Resolution MRS in the Presence of Field Inhomogeneity via Intermolecular Double-Quantum Coherences on a 3-T Whole-Body Scanner

Yanqin Lin,[1,4†] Tianliang Gu,[1†] Zhong Chen,[4] Scott Kennedy,[3] Mathews Jacob,[1,2] and Jianhui Zhong[1,2*]

Signals from intermolecular double-quantum coherences (iDQCs) have been shown to be insensitive to macroscopic field inhomogeneities and thus enable acquisition of high-resolution MR spectroscopy in the presence of large inhomogeneous fields. In this paper, localized iDQC ^{1}H spectroscopy on a whole-body 3-T MR scanner is reported. Experiments with a brain metabolite phantom were performed to quantify characteristics of the iDQC signal under different conditions. The feasibility of in vivo iDQC high-resolution MR spectroscopy in the presence of large intrinsic and external field inhomogeneity (in the order of hundreds of hertz) was demonstrated in the whole cerebellum of normal volunteers in a scan time of about 6.5 min. Major metabolite peaks were well resolved in the reconstructed one-dimensional spectra projected from two-dimensional iDQC acquisitions. Investigations on metabolite ratios, signal-to-noise ratio, and line width were performed and compared with results obtained with conventional point-resolved spectroscopy/MR spectroscopy in homogeneous fields. Metabolite ratios from iDQC results showed excellent consistency under different in vitro and in vivo conditions, and they were similar to those from point-resolved spectroscopy with small voxel sizes in homogeneous fields. MR spectroscopy with iDQCs can be applied potentially for quantification of gross metabolite changes due to diseases in large brain volumes with high field inhomogeneity. Magn Reson Med 63:303–311, 2010. ©2010 Wiley-Liss, Inc.

Key words: intermolecular double-quantum coherences (iDQCs); inhomogeneous broadening; high-resolution; localized spectroscopy; human cerebellum

In vivo magnetic resonance spectroscopy (MRS) allows noninvasive analysis of metabolites in humans. It is widely used for investigation of pathogenesis, monitoring metabolite responses, and clinical diagnosis of cancers and various neurologic diseases. However, magnetic field homogeneity in vivo is often degraded by magnetic susceptibility variation near, for example, air/tissue interfaces, bones and cerebrospinal fluid in brain, or with large interferences from fat and other fluid signals in the prostate. The field distortions can be as large as 2.0 part per million (ppm) over a $20 \times 20 \times 20$ mm^3 voxel (1) and are not well corrected with the 1st- and 2nd-order shimming available in most clinical MR scanners. Under such circumstances, spectra obtained by conventional MRS techniques are often poor and unusable. One way to remove the effect of inhomogeneous fields up to hundreds of hertz is to use techniques based on intermolecular multiple-quantum coherences that originate from dipole-dipole interactions between spins of different molecules. Intermolecular zero-quantum coherences (iZQCs) have been explored to obtain high-resolution spectra from nonlocalized controlled inhomogeneous samples (2–4) and biologic samples (5–7) at high magnetic fields. Localized iZQC spectra of living animals were also obtained on a 17.6-T spectrometer (8,9). In comparison to the iZQCs, previous studies indicate that pure intermolecular double-quantum coherence (iDQC) signals can be obtained without use of additional phase cycles, and their intensities are approximately 30% higher than those from iZQCs (10). Pulse sequences based on iDQCs such as intermolecular dipolar-interaction enhanced all lines (11) and its similar version (12) have been successfully utilized to obtain spectra with sharp resonance lines under controlled inhomogeneous fields. To increase the acquisition efficiency, an improved version of the pulse sequence (intermolecular dipolar-interaction enhanced all lines-II) has been developed as well (13).

In this study, the feasibility of in vivo high-resolution localized iDQC spectroscopy was investigated for the first time on a clinical scanner. A localized, two-dimensional (2D) iDQC pulse sequence based on intermolecular dipolar-interaction enhanced all lines-II was implemented on a 3-T whole-body scanner. Experiments with a brain metabolite phantom and whole cerebellum in human volunteers were performed. In the resulting one-dimensional (1D) spectra projected from 2D acquisitions obtained under 7 min, three major brain metabolite peaks, *N*-acetyl aspartate (NAA), creatine (Cr) and choline (Cho), were well resolved from volumes large enough to cover the entire cerebellum. Quantitative investigations on metabolite ratios, signal-to-noise ratio (SNR), and line width were performed as well.

[1]Department of Imaging Sciences, University of Rochester, Rochester, New York, USA.

[2]Department of Biomedical Engineering, University of Rochester, Rochester, New York, USA.

[3]Department of Biochemistry and Biophysics, University of Rochester, Rochester, New York, USA.

[4]Department of Physics and Fujian Key Laboratory of Plasma and Magnetic Resonance, State Key Laboratory of Physical Chemistry of Solid Surface, Xiamen University, Xiamen, China.

Grant sponsor: National Institutes of Health; Grant number: NS41048.
Grant sponsor: NNSF of China; Grant number: 10774125.

†These authors contributed equally to the work.

*Correspondence to: Jianhui Zhong, Ph.D., Department of Imaging Sciences, University of Rochester School of Medicine and Dentistry, Box 648, Elmwood Avenue, Rochester, NY 14642-8648.
E-mail: jianhui.zhong@rochester.edu

Received 20 May 2009; revised 31 August 2009; accepted 7 September 2009.

DOI 10.1002/mrm.22224
Published online in Wiley InterScience (www.interscience.wiley.com).

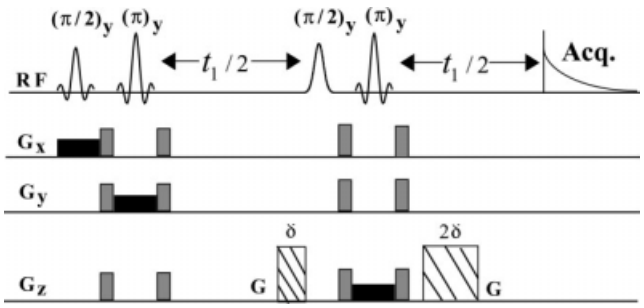

FIG. 1. 2D iDQC MRS pulse sequence with a PRESS localization module for localization. Sinc pulses are used for volume selection, signal excitation, and refocusing. The gaussian-shaped pulse is water selective. Gray rectangles stand for spoiler gradients, black rectangles stand for slice selection gradients, and dashed rectangles are CSGs for iDQCs. The refocusing gradient corresponding to the first sinc pulse is not shown.

THEORY

It has been reported that point-resolved spectroscopy (PRESS) (14) is the preferred localization method for acquisition of multiple spin echoes on a clinical 1.5-T scanner (15). The iDQC signal is of similar nature as multiple spin echoes, and the PRESS localization method was therefore adopted to localize the iDQC signal for this study. The standard PRESS sequence provided by the vendor was modified to construct the localized 2D iDQC pulse sequence (Fig. 1). The water suppression module in the original PRESS sequence was eliminated since water magnetization is needed to produce the dipolar field in the iDQC sequence. The radiofrequency pulses in PRESS were used for volume selection, signal excitation (the first sinc $\pi/2$ pulse in Fig. 1), and refocusing (the last sinc π pulse in Fig. 1). A gaussian shaped pulse was made frequency selective for the water resonance. A pair of gradients with the area ratio 1:2 along the z direction was employed as coherence selection gradients (CSGs) to select the iDQC signal. For all measurements in this study, CSGs were applied along the z direction. The total evolution time includes two intervals, one ($t_1/2$) before the gaussian pulse and the other ($t_1/2$) after the last sinc π pulse. These two intervals were incremented synchronously during the 2D iDQC experiment.

There are two different theoretical frameworks for analyzing long-range dipolar interactions in NMR spectroscopy: classic treatment (16) and quantum formalism (17). These frameworks, however, have been proven to be equivalent in nature (17,18). The quantum treatment, which is more direct for predicting coherence transfer pathways, is employed for illustrating the spin evolution of the localized 2D iDQC sequence shown in Fig. 1. Without loss of generality, a two-component sample system with spin species I and S is considered. It is assumed that the I component (corresponding to water) is abundant and S component (corresponding to brain metabolites) is dilute. Let ω_q be the frequency offset of spin q ($q = I, S$) in the rotating frame in the absence of field inhomogeneity. When the inhomogeneous field ΔB is taken into account, the frequency offset, Ω_q, of the q spin is given by

$$\Omega_q(r) = \omega_q + \Delta\omega(r) = \omega_q + \gamma\Delta B(r), (q = I, S), \quad [1]$$

where γ is the proton gyromagnetic ratio. Equation 1 suggests that the magnetic field inhomogeneity causes a shift of angular frequency from the resonance frequency ω_q.

For simplification, the effects of radiation damping, diffusion, relaxation, and scalar coupling are ignored, as are summations over all molecules in the sample (17). The magnetization density of the S component attributed to the observable signal during the detection period can be written as (13):

$$\sigma = -(i/8)S^{-}\sin[D_{IS}(0.5t_1 + t_2)]\exp(i\Omega_S t_2)\exp(-i\Omega_I t_1/2) \quad [2]$$

where D_{IS} is the residual intermolecular dipolar coupling constant and S^{-} is the lowering operator of the S spin and is equal to $S_x - iS_y$. Equation 2 shows that the iDQC cross-peak will be located at $(\Omega_I/2, \Omega_S) = [(\omega_I + \Delta\omega)/2, \omega_S + \Delta\omega]$. If the frequency offset of I is set to zero, i.e., $\omega_I = 0$, the peak will appear at $(\Delta\omega/2, \omega_S + \Delta\omega)$. This indicates that the spectral width in the F1 dimension can be as small as half the range of inhomogeneity. Compared to the conventional 2D intermolecular multiple-quantum coherence spectrum, which requires sampling of the whole range of chemical shift (11), this modification in the pulse sequence enables a substantial decrease of the F1 spectral width that needs to be sampled and thus greatly reduces the scan time and data size. In the inhomogeneous fields, due to the broadening of spectral peaks along both F1 and F2 dimension, all the peaks appear as separate streaks along the direction $\phi = \text{arctg}(2) = 63.4°$, where ϕ is the angle of spectral streaks with respect to the F1 axis. Although the ranges of the streaks in both F1 and F2 dimensions are susceptible to inhomogeneity, an accumulated projection of the cross-peaks onto the F2 dimension after counterclockwise rotating the streaks by ϕ results in a 1D high-resolution MRS without inhomogeneous broadening. In addition, it can be verified in Eq. 2 that chemical shift evolution of S component no longer exists in the t_1 period due to the refocusing π pulse inserted in the middle t_1 evolution period, similar to 2D J-resolved spectra.

MATERIALS AND METHODS

All experiments were carried out on a Siemens 3-T Trio whole-body scanner (Siemens Medical Solution, Erlangen, Germany) running 2004A software, with a standard circular polarization (CP) birdcage head coil for radiofrequency excitation and signal reception. The gradient system was capable of producing an amplitude of 40 mT/m along each axis of the laboratory coordinate system within a minimal rise time of 200 μs. Integrated Development Environment for Applications, provided by the vendor, was used for the iDQC pulse sequence programming. The selective $\pi/2$ gaussian pulse in Fig. 1 for water resonance had a width of 8 ms and was frequency selective for water. The CSG was applied with strength G of 20 mT/m and duration δ of 3000 μs unless otherwise specified. The raw data produced by localized 2D iDQC sequence were saved and processed using homemade

software based on Matlab 6.5.0 (The Mathworks Inc., Natick, MA, USA). A sine-bell-shaped low-pass filter was used for water suppression (19). As indicated in the "Theory" section, all metabolite peak streaks in the 2D spectra extended along the direction of 63.4° relative to the F1 axis. Therefore, metabolite streaks were rotated counterclockwise by 63.4° and then accumulatively projected onto the F2 axis to generate high-resolution 1D spectra. To maintain consistency for easy comparison, the data acquired with standard PRESS sequence were also processed using the same software. All 2D and 1D iDQC and PRESS spectra were displayed in the magnitude mode. In order to reach the steady state for magnetization, four dummy scans were acquired. In order to reduce the system errors and investigate the reliability of iDQC method at the same time, both iDQC and PRESS experiments were repeated three times. The SNR was calculated by dividing the peak intensity of NAA by the standard deviation (SD) of signal in the region between 7.0 and 8.0 ppm. Line width of the water peak was measured during the shimming process. Line width of the NAA peak was measured as full width at half maximum in the obtained 1D spectrum. Comparisons of metabolite ratios, SNR, and line width were performed.

Phantom Experiments

A proton MRS brain phantom with cylindrical shape and metabolite composition (20) and size similar to that of a normal human brain was used to investigate the signal property of iDQC in a 3.0-T clinical scanner. The concentrations of three major metabolites, NAA, Cr, and Cho, are 12.5, 10.0, and 3.0 mM, respectively. For data acquisition with the localized 2D iDQC pulse sequence, the F1 spectral width was 250 Hz (t_1 step size of 4 ms) in 128 increments unless otherwise specified, and the F2 spectral width was 1000 Hz. The pulse repetition time was 1500 ms and the acquisition time t_2 was 1000 ms. Echo time/2 corresponding to the second π pulse ranged from about 10 to 266 ms. Total experimental time was 3 min 18 sec. The signal was zero filled to 1024×4096 before a regular fast fourier transform (FFT) process. For PRESS experiments, pulse repetition time and echo time were 1500 and 135 ms, respectively. A long echo time was chosen in order to reduce signal from metabolites of short T2, thus facilitating clear spectral identification of resonance peaks from three major metabolites (NAA, Cr, and Cho). The number of averages was 64. The acquisition time t_2 was 1000 ms, with a spectral width of 1000 Hz. The total experimental time was 1 min 42 sec. The signal was zero filled to 4096 before a regular FFT process. Here, in order to saving acquisition time, a relatively short pulse repetition time of 1500 ms was used as in the study by Schirmer and Auer (20). Therefore, the relative metabolite ratios are weighted by T_1 values of metabolites for both PRESS and iDQC methods.

MR signal intensity is directly proportional to the voxel magnetization; thus, an increase in the voxel volume should increase the signal intensity if other experimental conditions are kept the same. Two experiments were performed to investigate how signals vary with different voxel sizes. In the first experiment, in order to investigate the immunity of iDQC signal for field inhomogeneity with different voxel volumes, voxel sizes of $70 \times 70 \times 70$, $60 \times 60 \times 60$, $50 \times 50 \times 50$, and $40 \times 40 \times 40$ mm^3 were chosen, with the volumes located at the magnet isocenter. The magnetic field was intentionally deshimmed by adjusting the y shim coil in all phantom experiments to produce a line width of about 60 Hz for the water resonance at voxel size $70 \times 70 \times 70$ mm^3, and the same shimming was maintained for all iDQC experiments with different voxel sizes. In the second experiment, voxel sizes of $70 \times 70 \times 70$, $60 \times 60 \times 60$, $50 \times 50 \times 50$, and $40 \times 40 \times 40$ mm^3 were chosen with the same line width of water resonance and with volumes at the isocenter in inhomogeneous fields. The water line width was kept at about 30 Hz by manually adjusting the shimming before measurements with each voxel volume. For comparison with the iDQC measurements, PRESS measurements were performed on the phantom in homogeneous fields to obtain reasonable spectral resolution. Voxel sizes of $10 \times 10 \times 10$, $20 \times 20 \times 20$, $30 \times 30 \times 30$, and $40 \times 40 \times 40$ mm^3 were used with volumes at the isocenter and with the same T_2^* that was measured in the shimming process.

iDQC signal originates mainly from the spins within the dipolar correlation distance to each other. Therefore, dipolar correlation distance, defined as $d_c = \pi/\gamma G\delta$ (where G and δ are amplitude and duration of CSG, respectively), is an important parameter in iDQC experiments. iDQC experiments were performed using a volume of fixed size $60 \times 60 \times 60$ mm^3, with fixed CSG amplitude of 20 mT/m in an inhomogeneous field (with line width of water resonance of about 40 Hz) but different durations of CSG of 1, 2, 3, 4, 5, and 6 ms, corresponding to the dipolar correlation distance of 587, 293, 196, 147, 118, and 98 μm, respectively. By setting different initial t_1 (0) evolution times for different experiments with different durations of CSG, the total t_1 evolution time of these experiments was kept the same.

One of the distinct advantages of iDQC signal lies in its insensitivity to the inhomogeneous magnetic fields. In order to study the influence of inhomogeneous fields, iDQC experiments were carried out within a fixed voxel size $60 \times 60 \times 60$ mm^3 under different inhomogeneous fields, with the line widths of water resonance adjusted to about 7, 20, 30, 40, 50, 60, 70, 80, 90, 100, 110, 120, 130, 140, and 150 Hz, respectively.

Total experimental time is critical for a clinical study. Long acquisition time needed for a 2D measurement is often an obstacle for its clinical applications. Due to refocusing of chemical shifts of metabolite in the indirect (F1) dimension with the sequence in Fig. 1, only half the range of inhomogeneous broadening needs to be sampled, which can be much smaller than that in the direct (F2) dimension, and thus the acquisition efficiency can be improved greatly. In order to evaluate the time efficiency of the sequence, a measurement was performed to evaluate how fast an acceptable 2D spectrum can be obtained in a fixed voxel size $60 \times 60 \times 60$ mm^3 with an inhomogeneous field of water line width of about 30 Hz.

Human Volunteer Experiments

Experiments on human cerebellum were performed to demonstrate the possibility of iDQC high-resolution MRS

in vivo on a clinical scanner. Five healthy volunteers (age 39 ± 8 years; one female) were examined. Informed prior consent was approved by the research board of University of Rochester and agreed to by all volunteers.

For the 2D iDQC experiments, a 40 × 40 × 80 mm^3 voxel was prescribed to cover the whole cerebellum (with left/right dimension 80 mm, as shown in Fig. 6c) after multiple-slice three-plane localization. For most subjects, this volume also covers some interfacing structures surrounding the cerebellum, such as cerebrospinal fluid and skull bones. No manual shimming was applied, and thus the time for manual shimming always required by conventional MRS technique was saved. The spectral width of the F1 dimension was 500 Hz (t_1 step size of 2 ms) in 128 increments and was 1000 Hz for the F2 dimension. The pulse repetition time was 3000 ms and the acquisition time t_2 was 1000 ms. The total experimental time was about 6.5 min. The signal was zero filled to 2048 × 4096 before a regular FFT process. For PRESS experiments, manual 1st- and 2nd-order shimming was performed. Larger voxels were more difficult to shim and had larger line widths for the major metabolite peaks. It was found that the Cr and Cho peaks overlapped each other when voxel size reached 30 × 30 × 30 mm^3, and no quantifiable spectra can be obtained at voxel size 40 × 40 × 40 mm^3. Therefore, a 20 × 20 × 20 mm^3 voxel (as shown in Fig. 6a) was chosen for quantification due to its higher SNR over results from voxel size 10 × 10 × 10 mm^3. Pulse repetition time and echo time were 3000 and 30 ms, respectively. Short echo time was applied for higher signal intensity. The number of average was 96. The acquisition time t_2 was 1000 ms, with a spectral width of 1000 Hz. The total experimental time was about 5 min, not including the time for manual shimming.

RESULTS AND DISCUSSION

The resonance peak height (or area) in MRS is directly proportional to the concentration of metabolites. When in vivo tissue is abnormal, concentrations of metabolites often change. It is reported that NAA reduces significantly in the cerebellum of patients with cerebellar degeneration (21) and familial hemiplegic migraine type 1 (22). Although absolute concentration measurement of metabolite is important, many studies do not attempt to quantify absolute metabolite concentrations, but rather report relative ratio of each metabolite, often using Cr as a reference (23). Quantification based on metabolite ratio was adopted in this study. Metabolite ratios were calculated by dividing integrals of the peak area of NAA and Cho by that of Cr.

Phantom Study Results

It is known that with conventional MRS techniques such as PRESS, the line widths of spectral peaks increase when magnetic field homogeneity decreases. This results in overlap of metabolite peaks, and little useful information can be obtained when the inhomogeneity is larger than separations between the peaks. Figure 2a shows a PRESS spectrum obtained in an inhomogeneous field with the water line width of about 45 Hz from a voxel of

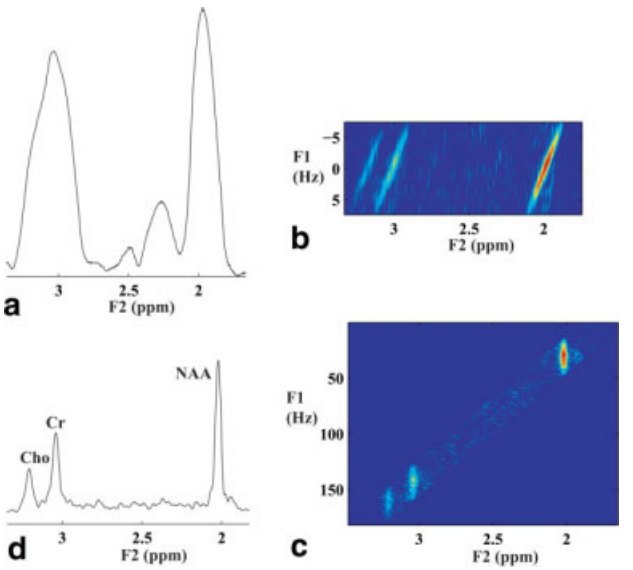

FIG. 2. Spectra of the metabolite phantom obtained from a voxel of 50 × 50 × 50 mm^3 in an inhomogeneous field. **a:** PRESS spectrum, (**b**) the original iDQC 2D spectrum using the sequence in Fig. 1, (**c**) counterclockwise rotation of (**b**) by 63.4°, and (**d**) accumulated projection onto F2 dimension from (**c**). [Color figure can be viewed in the online issue, which is available at www.interscience.wiley.com.]

50 × 50 × 50 mm^3. Cho and Cr peaks are completely overlapped, making the reliable measurements of chemical shifts and metabolite ratios almost impossible. iDQC was also performed in the same inhomogeneous field. Figure 2b is the original 2D spectrum. Figure 2c is obtained by rotating the spectrum in Fig. 2b counterclockwise by 63.4°, as indicated in the "Theory" section. Figure 2d is the accumulated projection from Fig. 2c. The line width of NAA is about 23 Hz in Fig. 2a but only about 5 Hz in Fig. 2d. Comparing Fig. 2d to Fig. 2a, the resolution increases greatly and three major metabolite peaks can be clearly resolved. It suggests that iDQC can produce narrow line shapes under inhomogeneous magnetic fields. Therefore, reliable quantification can be performed using the results in Fig. 2d, but not Fig. 2a.

Quantitative results from different voxel sizes under the same shimming are presented in Fig. 3a and b. From Fig. 3a, metabolite ratio NAA/Cr remains at about 1.50 and Cho/Cr varies between 0.65 and 0.70 in spite of variation of the voxel size. The metabolite ratio is not quantifiable when the voxel size is smaller than 64,000 mm^3 (40 × 40 × 40 mm^3) for the iDQC measurements due to low signal intensity. From Fig. 3b, signal increases proportionally with the increase in voxel volume. This trend is similar to that reported in previous work (24). However, SNR decreases more quickly with the decrease of voxel volume, as reported in that study. The discrepancy may be due to the existence of an additional local dipole field generated by the glass sphere in the isocenter of the sample in that study. Although the line widths of water peak from conventional technique increased with the voxel volume, the line widths of NAA peak from 1D iDQC projection spectra remain almost unchanged, at about 5.5 Hz. The line width of NAA peak from

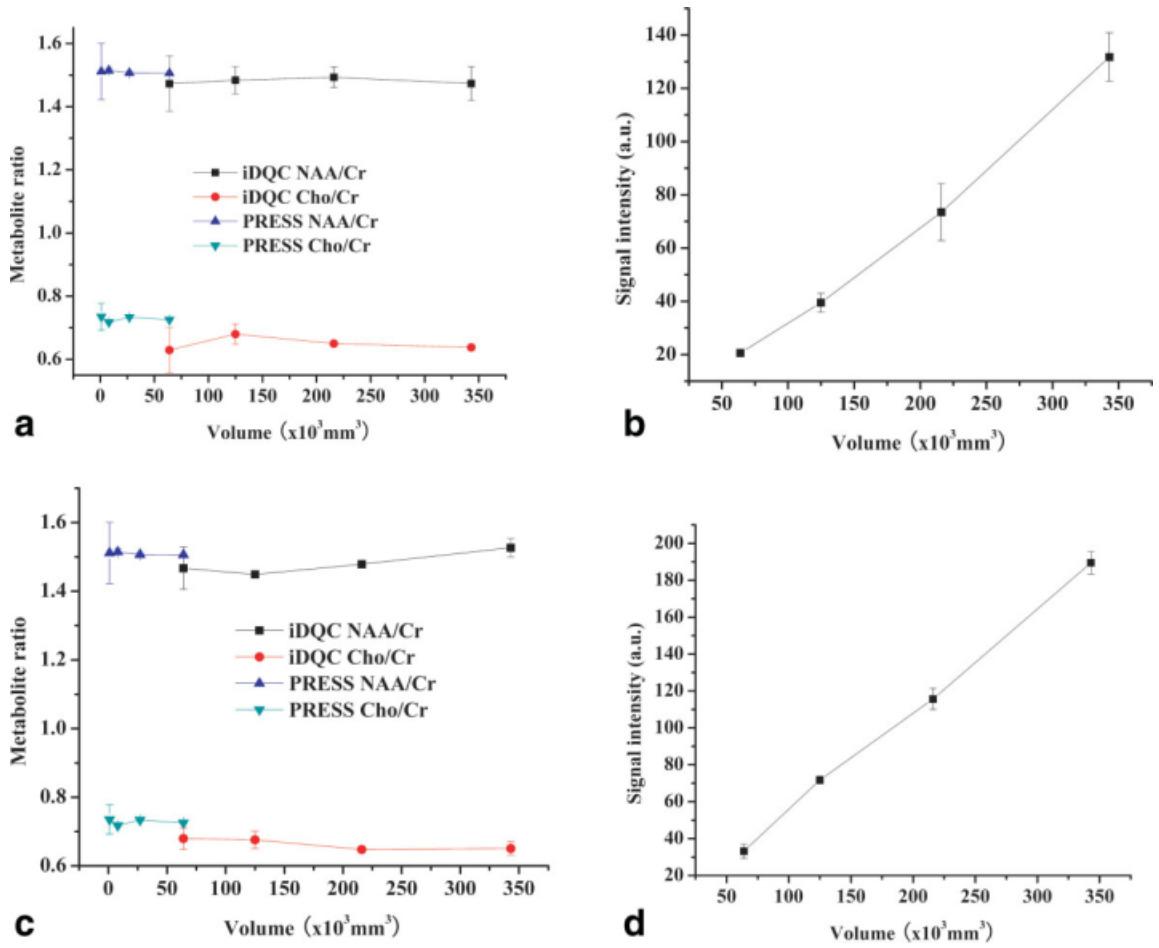

FIG. 3. Properties of iDQC signals of the phantom under different voxel sizes, with the same shimming resulting in different line width of water resonance at different voxel sizes (**a,b**) and with the same line width of water resonance at different voxel sizes (**c,d**). **a,c:** Metabolite ratios. **b,d:** Signal intensity of NAA under these conditions. The metabolite ratios from PRESS measurements under different voxel sizes in the homogeneous fields are also included for comparison. The SD from three measurements was represented as error bars; a.u. = arbitrary unit. [Color figure can be viewed in the online issue, which is available at www.interscience.wiley.com.]

corresponding PRESS spectra under the same experimental conditions increases with the volume. Figure 3c and d shows the iDQC signal properties under different voxel size but with the same water line width. Metabolite ratio NAA/Cr is about 1.50, while Cho/Cr is close to 0.70, even when the voxel size is changed. The iDQC signal intensity in Fig. 3d shows similar trend as Fig. 3b, increasing with the volume. Figure 3 also shows metabolite ratios from standard PRESS in homogeneous fields. NAA/Cr is about 1.50 and Cho/Cr about 0.7. Figure 3 suggests that the metabolite ratios from iDQC measurements with large voxel sizes in inhomogeneous fields are very similar to that from PRESS measurements with small voxel sizes in homogenous fields.

Metabolite ratio of NAA/Cr remains at about 1.50 and Cho/Cr about 0.6 when the CSG is varied, as shown in Fig. 4a. Figure 4b shows signal intensity variation with CSG from the experimental and theoretical data. It is observed that iDQC signal is attenuated with increasing of CSG. A similar trend was reported in previous studies (25,26). The theoretical curve of signal intensity of NAA in pure water (labeled as "Theoretical (water)" in Fig. 4b) results from fitting the experimental data with the expression in Eq. 4 in (25). The theoretical curve of signal intensity of NAA in tissue (labeled as "Theoretical (tissue)" in Fig. 4b) was generated with the assumption that signal intensity of NAA in pure water and tissue is the same when the CSGs are equal to zero but diffusion coefficient of NAA in tissue is about one third of that in pure water. It clearly shows that CSG plays a role in signal attenuation due to diffusion. However, this attenuation is small for typical correlation distances. For the dipolar correlation distance of 196 μm used in this study (marked by an arrow in Fig. 4b), the signal attenuation is about 8%, 9%, and 3% for experimental data, theoretical data in water, and theoretical data in tissue, respectively. From Fig. 4c, it is seen that metabolite ratio of NAA/Cr remains at about 1.50 and Cho/Cr between 0.6 and 0.65 under different inhomogeneous magnetic fields indicated by line width of water. In Fig. 4d, signal intensity slightly decreases with the increase of the line width. The line widths of NAA peak from 1D projection spectra are around 5.5 Hz, although the iDQC acquisition is performed under different inhomogeneous magnetic fields. Metabolite ratio of NAA/Cr obtained from iDQC spectra ranges from 1.45 to 1.55 and Cho/Cr from 0.60 to 0.70

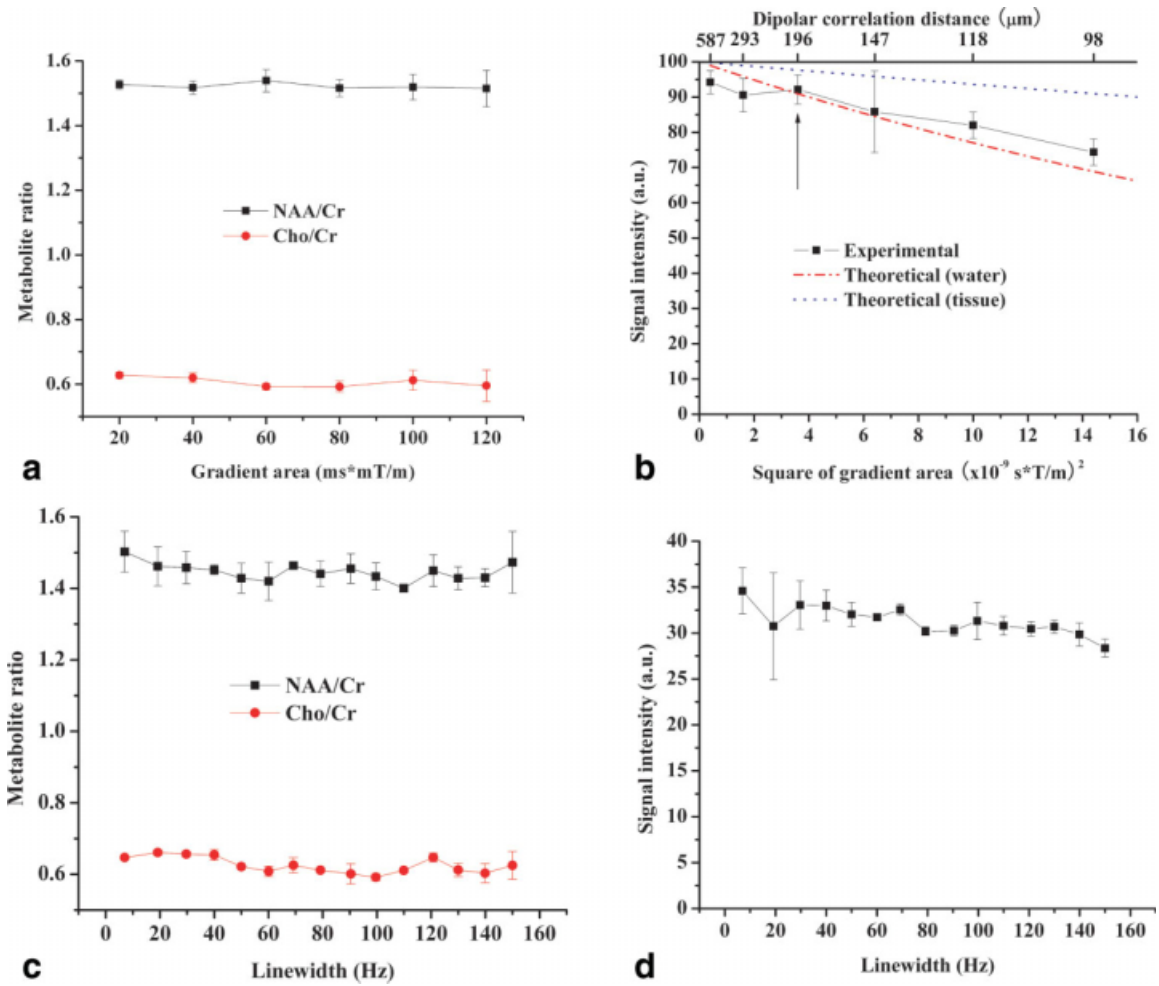

FIG. 4. Properties of iDQC signals of the phantom at a fixed voxel size of 60 × 60 × 60 mm^3 under different areas of CSGs (**a,b**) and under different line widths of water (**c,d**). **a,c:** Metabolite ratios. **b,d:** Signal intensity of NAA. In (**b**), "Theoretical (water)" is for theoretical values of NAA in pure water, while "Theoretical (tissue)" is for theoretical values of NAA in tissue. The signal intensity of theoretical data is set to 100 when CSG equals zero. See the text for details. The SD from three measurements was represented as error bars; a.u. = arbitrary unit. [Color figure can be viewed in the online issue, which is available at www.interscience.wiley.com.]

under conditions with large variations in voxel volumes, field inhomogeneity, and CSGs. The fact that variation of metabolite ratios and SD remains within a small range suggests that iDQC can potentially be a feasible technique to quantify metabolite ratio in inhomogeneous fields and a reliable method for MRS applications in a clinical scanner.

The results for test of acquisition time efficiency are shown in Fig. 5. The spectrum of Fig. 5a was obtained with the F1 spectral width of 50 Hz in nine t_1

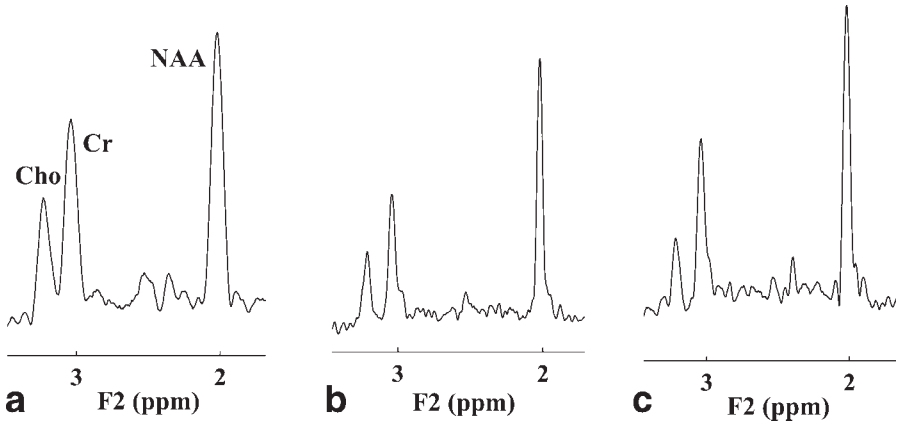

FIG. 5. iDQC spectra from the metabolite phantom, with (**a**) nine and (**b**) 25 t_1 increments in the F1 spectral width of 50 Hz, (**c**) with nine t_1 increments in the F1 spectral width of 25 Hz.

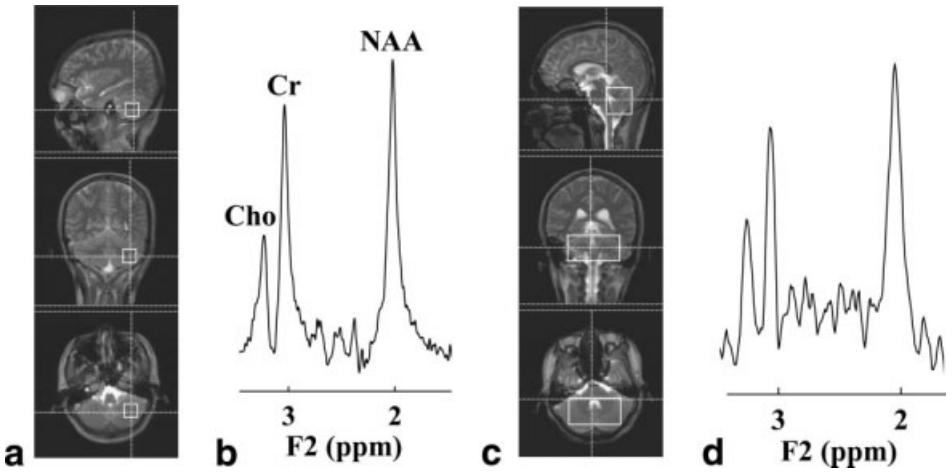

FIG. 6. Typical in vivo spectra in the human cerebellum. **a:** Voxel position with a voxel size of 20 × 20 × 20 mm^3 displayed on anatomic images of three orientations and (**b**) the corresponding PRESS spectrum. **c:** Voxel position of a voxel of 40 × 40 × 80 mm^3 displayed on anatomic images of three orientations and (**d**) corresponding 1D iDQC projection spectrum.

increments. The total acquisition time including the time used for four dummy scans was 20 sec. Figure 5b was acquired in 25 t_1 increments, with a total acquisition time of 44 sec. The line widths of NAA peak are 12.59 and 5.91 Hz in Fig. 5a and b respectively, and the SNR efficiencies, defined as SNR per (scan time in minutes)$^{1/2}$ are 65.42 and 55.15, respectively. The dependence of line width and SNR efficiency on numbers of t_1 increment follows the same trend as that in a previous study (8). Figure 5c was acquired with the F1 spectral width of 25 Hz in nine t_1 increments. The acquisition time was the same as Fig. 5a. The line width of NAA peak is 7.49 Hz in Fig. 5c and SNR efficiency is 61.50. Comparing Fig. 5c to Fig. 5a, the spectral resolution is improved without increasing acquisition time but the SNR efficiency is decreased. Compared to localized 2D iZQC sequences, which require at least full chemical shift range of solute for the F1 spectral width (8), the minimal spectral width in the F1 dimension for the iDQC sequence in Fig. 1 can be half the range of the inhomogeneous magnetic field, which is usually much smaller than the full chemical shift range of solute. It means that fewer t_1 steps for iDQC can be applied for the same resolution, and thus time efficiency can be improved substantially.

Human Volunteer Results

The conventional PRESS 1D spectrum from a 20 × 20 × 20 mm^3 voxel of one subject is shown in Fig. 6b, with the position of the voxel indicated in Fig. 6a on the T_1-weighted anatomic images along three orientations. The voxel is located near the center of the right cerebellum for a relatively homogeneous magnetic field. The three major metabolite peaks can be clearly identified. Figure 6c shows the location of a 40 × 40 × 80 mm^3 voxel covering the whole left and right cerebellum of the same subject used for the iDQC acquisition. It is noted that the voxel not only contains the cerebellum tissue but also cerebrospinal fluid and partially interfaces with the brain with the skull bony structures. A high-resolution 1D projection spectrum with similar resolution as Fig. 6a was generated, as shown in Fig. 6d. The line with of NAA peak in the projected spectrum is about 6.0 Hz. The total scan time is about 6.5 min, which is acceptable for clinical application. This result suggests that the iDQC method is promising for obtaining high-resolution in vivo spectra in the presence of large field inhomogeneity that is often not feasible with conventional MRS techniques. The metabolite ratios of the five human subjects from iDQC and PRESS measurements are shown in Fig. 7, with the mean value and the SD from three measurements for each subject represented as error bars. It can be seen that metabolite ratios from PRESS and iDQC measurements are comparable to each other, with maximal difference less than 20%.

Conventional (intramolecular) double-quantum filters have been utilized for suppression of strong singlets and optimal detection of J-coupled resonance, such as γ-aminobutyric acid (27,28) and glutathione (29,30). Since intramolecular double-quantum coherences originate from J-coupling interaction, non-J-coupled spins give no signal. On the other hand, since iDQCs come from long-range dipolar coupling between water and metabolite spins, both J-coupled and non-J-coupled spins experience the same dipolar field and result in detectable

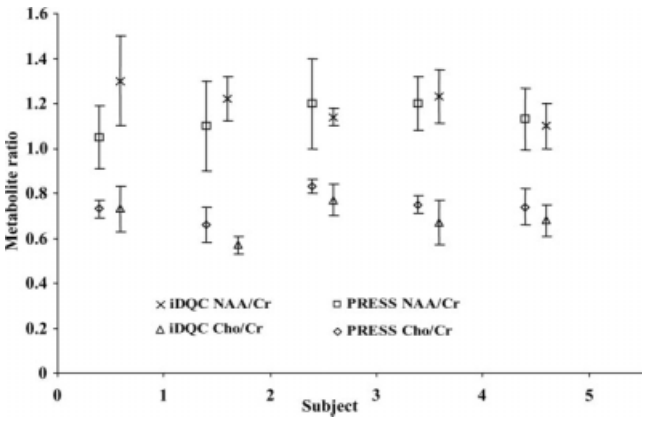

FIG. 7. Metabolite ratios of in vivo PRESS spectra from voxels of 20 × 20 × 20 mm^3 and iDQC spectra from voxels of 40 × 40 × 80 mm^3 on human cerebellums of five normal volunteers. The data with the mean and SD calculated from three measurements in each subject are shown.

signals. In the iDQC spectra obtained with the pulse sequence in Fig. 1, the J-scaling factor is 3. This benefits the weakly coupled system for accurate measurement of small J coupling constant but aggravates the overlapping of metabolite peaks from strongly coupled spins.

There are clinical cases where acquisition of brain MRS in a large volume is very helpful. Small volume of interest can suffer from problems of partial coverage and uncertainty in the reproducibility of the placement of volume of interest in serial studies (31,32). An iDQC method that acquires from a large voxel can significantly alleviate this issue. In addition to the whole cerebellum studies demonstrated in this paper, the 2D iDQC MRS method can be useful for tumor studies, tissue investigation shortly after surgery, and for other brain regions close to air cavities, bones, or cerebrospinal fluid, such as brain stem, where large intrinsic field inhomogeneity exists. Conventional MRS techniques often fail in these regions, even with time-consuming 1st- and 2nd-order manual shimming. However, the SNR of iDQC signal is intrinsically low, equal to only a few percent of the conventional SQC. In the current 3-T study, only strong singlets can be reliably detected due to the limited SNR at 3 T. This does not lead to state-of-art clinical applications. Therefore, the iDQC method is not recommended when a conventional method works well. The iDQC method, however, can be a complementary technique where conventional methods fail in the presence of large field inhomogeneity. To compensate partially for the low SNR, a large voxel can be prescribed in iDQC measurements to cover the whole region of interest. In addition, scans performed in the higher magnetic field such as 7 T (33) can improve iDQC SNR substantially.

The existence of local inhomogeneity (such as additional local field gradients due to magnetic susceptibility variations) can affect the overall dipolar field and effectiveness of the externally applied CSGs in selecting iDQC signal. It is known that iDQC signal comes mainly from spins within the dipolar correlation distance that is typically much smaller than the voxel size. If the CSG is large compared to the local field within the dipolar correlation distance, the local field variation will have minimal effects on the field homogeneity. In this case, iDQC signal will be mostly independent of local inhomogeneity. On the other hand, field inhomogeneity within the correlation distance will still have effects on the obtained signal. In the case of strong local field such as in the presence of strong local dipolar field, as reported in a previous study (24), detection of iZQC signal becomes impossible. This also holds true for iDQC. Moreover, if metabolites are distributed nonuniformly in space, the resulting average metabolite ratio is also weighted by the local variation of metabolite. A similar effect holds for conventional PRESS, except that the dipolar correlation distance used for iDQC (198 μm in our case) is usually much smaller than the typical voxel size in PRESS, so the effect of microscopic susceptibility will be less with iDQC. The application of the proposed iDQC technique is likely limited to the case where a global estimation of metabolites is more relevant (i.e., overall metabolic status and its change as a disease progresses) than local distributions of metabolites. Localized iDQC spectra suffer from chemical shift artifact just like the PRESS technique. In the current work, Cr and NAA overlap for 85.6%, and Cr and Cho for 97.1%, when only the singlets of NAA at 2.02 ppm, Cr at 3.04 ppm, and Cho at 3.24 ppm are considered (34).

CONCLUSIONS

A localized 2D iDQC pulse sequence was implemented on a 3-T clinical scanner and applied for MRS in both a brain metabolite phantom and the normal human cerebellum for the first time. The method holds the advantage of immunity to magnetic field inhomogeneity and high acquisition efficiency, which results in the capability to obtain high-resolution spectra in a few minutes. It is shown that the iDQC spectrum acquired from large voxels and under highly inhomogeneous field has a resolution similar to that of the conventional PRESS spectrum acquired in a smaller, homogeneous volume. The three major brain metabolite peaks can be clearly resolved in the 1D spectrum projected from the 2D iDQC acquisition. Moreover, metabolite ratios from iDQC results show excellent consistency under different in vitro and in vivo conditions. The results are similar to those from the conventional MRS method with small voxel sizes in homogeneous fields. The iDQC MRS may be applied to acquisition of high-resolution spectra and used for quantification of metabolites in large brain volumes with high field inhomogeneity, providing metabolic biomarkers for detection and diagnosis of cancers, metabolic diseases, and various neurologic disorders.

ACKNOWLEDGMENTS

One of the authors (Y. L.) is grateful to the China Scholarship Council for a fellowship.

REFERENCES

1. Li S, Dardzinski BJ, Collins CM, Yang QX, Smith MB. Three dimensional mapping of the static field inside the human head. Magn Reson Med 1996;36:705–714.
2. Vathyam S, Lee S, Warren WS. Homogeneous NMR spectra in inhomogeneous fields. Science 1996;272:92–96.
3. Chen Z, Hou T, Chen ZW, Hwang DW, Hwang LP. Selective intermolecular zero-quantum coherence in high-resolution NMR under inhomogeneous fields. Chem Phys Lett 2004;386:200–205.
4. Balla D, Faber C. Solvent suppression in liquid state NMR with selective intermolecular zero-quantum coherences. Chem Phys Lett 2004;393:464–469.
5. Faber C, Pracht E, Haase A. Resolution enhancement in in vivo NMR spectroscopy: detection of intermolecular zero-quantum coherences. J Magn Reson 2003;161:265–274.
6. Galiana G, Branca RT, Warren WS. Ultrafast intermolecular zero quantum spectroscopy. J Am Chem Soc 2005;127:17574–17575.
7. Chen X, Lin MJ, Chen Z, Cai SH, Zhong JH. High-resolution intermolecular zero-quantum coherence spectroscopy under inhomogeneous fields with effective solvent suppression. Phys Chem Chem Phys 2007;9:6231–6240.
8. Balla DZ, Melkus G, Faber C. Spatially localized intermolecular zero-quantum coherence spectroscopy for in vivo applications. Magn Reson Med 2006;56:745–753.
9. Balla DZ, Faber C. In vivo intermolecular zero-quantum coherence MR spectroscopy in the rat spinal cord at 17.6 T: a feasibility study. MAGMA 2007;20:183–191.
10. Zhong JH, Chen Z, Kwok E. In vivo intermolecular double-quantum imaging on a clinical 1.5 T MR scanner. Magn Reson Med 2000;43:335–341.

11. Chen Z, Chen ZW, Zhong JH. High-resolution NMR spectra in inhomogeneous fields via IDEAL (intermolecular dipolar-interaction enhanced all lines) method. J Am Chem Soc 2004;126:446–447.
12. Lin YQ, Chen ZW, Cai CB, Chen Z. High-resolution NMR spectra under inhomogeneous fields via intermolecular double-quantum coherences. Spectrochim Acta A 2008;70:1025–1028.
13. Chen Z, Cai SH, Chen ZW, Zhong JH. Fast acquisition of high-resolution NMR spectra in inhomogeneous fields via intermolecular double-quantum coherences. J Chem Phys 2009;130:084504.
14. Bottomley PA. Selective volume method for performing localized MR spectroscopy. U.S. patent 1984;4480228.
15. Bifone A, Payne GS, Leach MO. In vivo multiple spin echoes. J Magn Reson 1998;135:30–36.
16. Bowtell R, Bowley RM, Glover P. Multiple spin echoes in liquids in a high magnetic field. J Magn Reson 1990;88:643–651.
17. Lee S, Richter W, Vathyam S, Warren WS. Quantum treatment of the effects of dipole-dipole interactions in liquid nuclear magnetic resonance. J Chem Phys 1996;105:874–900.
18. Jeener J. Equivalence between the "classical" and the "Warren" approaches for the effects of long range dipolar couplings in liquid nuclear magnetic resonance. J Chem Phys 2000;112:5091–5094.
19. Marion D, Ikura M, Bax A. Improved solvent suppression in one- and two-dimensional NMR spectra by convolution of time-domain data. J Magn Reson 1989;84:425–430.
20. Schirmer T, Auer DP. On the reliability of quantitative clinical magnetic resonance spectroscopy of the human brain. NMR Biomed 2000;13:28–36.
21. Tedeschi G, Bertolino A, Massaquoi SG, Campbell G, Patronas NJ, Bonavita S, Barnett AS, Alger JR, Hallett M. Proton magnetic resonance spectroscopic imaging in patients with cerebellar degeneration. Ann Neurol 1996;39:71–78.
22. Dichgans M, Herzog J, Freilinger T, Wilke M, Auer DP. ^{1}H-MRS alterations in the cerebellum of patients with familial hemiplegic migraine type 1. Neurology 2005;64:608–613.
23. Barker PB, Lin DDM. In vivo proton MR spectroscopy of the human brain. Prog Nucl Magn Reson Spectrosc 2006;49:99–128.
24. Balla DZ, Faber C. Intermolecular zero-quantum coherence NMR spectroscopy in the presence of local dipole fields. J Chem Phys 2008;128:154522.
25. Kennedy SD, Zhong JH. Diffusion measurements free of motion artifacts using intermolecular dipole-dipole interactions. Magn Reson Med 2000;52:1–6.
26. Cai CB, Lin YQ, Cai SH, Chen Z, Zhong JH. High-resolution NMR spectra in inhomogeneous fields utilizing the CRAZED sequence without coherence selection gradients. J Magn Reson 2008;193:94–101.
27. Keltner JR, Wald LL, Frederick BD, Renshaw PF. In vivo detection of GABA in human brain using a localized double-quantum filter technique. Magn Reson Med 1997;37:366–371.
28. Choi CH, Coupland NJ, Hanstock CC, Ogilvie CJ, Higgins ACM, Gheorghiu D, Allen PS. Brain γ-aminobutyric acid measurement by proton double-quantum filtering with selective J rewinding. Magn Reson Med 2005;54:272–279.
29. Zhao TJ, Heberlein K, Jonas C, Jones DP, Hu XP. New double quantum coherence filter for localized detection of glutathione in vivo. Magn Reson Med 2006;55:676–680.
30. Choi CH, Zhao CG, Dimitrov I, Douglas D, Coupland NJ, Kalra S, Hawesa H, Davis J. Measurement of glutathione in human brain at 3T using an improved double quantum filter in vivo. J Magn Reson 2009;198:160–166.
31. Gonen O, Viswanathan AK, Catalaa I, Babb J, Udupa J, Grossman RI. Total brain N-acetylaspartate concentration in normal, age-grouped females: quantitation with non-echo proton NMR spectroscopy. Magn Reson Med 1998;40:684–689.
32. Falini A, Bozzali M, Magnani G, Pero G, Gambini A, Benedetti B, Mossini R, Franceschi M, Comi G, Scotti G, Filippi M. A whole brain MR spectroscopy study from patients with Alzheimer's disease and mild cognitive impairment. Neuroimage 2005;26:1159–1163.
33. Vaughan JT, Garwood M, Collins CM, Liu W, DelaBarre L, Adriany G, Andersen P, Merkle H, Goebel R, Smith MB, Ugurbil K. 7T vs. 4T: RF power, homogeneity, and signal-to-noise comparison in head images. Magn Reson Med 2001;46:24–30.
34. de Graaf RA, Rothman DL. In vivo detection and quantification of scalar coupled ^{1}H NMR resonances. Concept Magn Reson 2001;13:32–76.